

Supporting Information for:

**Rapid Metal-Catalyzed Hydrodehalogenation
of Iodinated X-Ray Contrast Media**

Lindsay E. Knitt^{a,c}, John R. Shapley^{b,c}, and Timothy J. Strathmann^{a,c*}

^aDepartment of Civil and Environmental Engineering, University of Illinois at Urbana-Champaign, Urbana, IL, 61801. ^bDepartment of Chemistry, University of Illinois at Urbana-Champaign, Urbana, IL 61801.

^cCenter of Advanced Materials for the Purification of Water with Systems, Urbana, IL 61801

*Corresponding author email: strthmnn@uiuc.edu

October 2007

11 Pages

6 Sections

2 Tables

6 Figures

Section S1. Chemical Reagents

All reagents used were of the highest purity available. Diatrizoate (2,4,6-triiodo-3,5-diacetamidobenzoate, sodium salt; Dia-I₃) and its non-iodinated analogue (3,5-diacetamidobenzoic acid; Dia-H₃), NaOH, NaClO₄, NaF, NaCl, NaBr, NaI, Na₂SO₄, NaNO₃, Na₂S, CaCl₂, MgCl₂, NaH₂PO₄, Na₂HPO₄, triethylamine, and ammonium acetate were purchased from Sigma-Aldrich-Fluka. Methanol, acetonitrile, and NaHCO₃ were purchased from Fisher Scientific. Iopromide was generously supplied by Schering AG (Berlin, Germany). Natural organic matter isolated from the Suwannee River (Okefenokee National Wildlife Refuge, GA) by reverse osmosis was obtained from the International Humic Substances Society. NaOCl solutions used for catalyst regeneration experiments were prepared from a 6% Clorox bleach mixture. Granular activated carbon was obtained from Calgon (type F-400, 840–1400 µm size fraction).

Section S2. Analytical Method Details

Aqueous samples were analyzed with high performance liquid chromatography-UV photodiode array detection (Shimadzu VP Series) to quantify the disappearance of diatrizoate (Dia-I₃; λ = 237 nm) and iopromide (Iop-I₃; λ = 241 nm), and formation of organic reaction intermediates and products (Dia-HI₂, λ = 234 nm; Dia-H₂I, λ = 253 nm; Dia-H₃, λ = 229 nm; Iop-HI₂, λ = 236 nm; Iop-H₂I, λ = 257 nm; Iop-H₃, λ = 217 nm;). Authentic standards were only available to quantify concentrations of the parent compounds (Dia-I₃ and Iop-I₃) as well as the deiodinated product of diatrizoate reduction (Dia-H₃). For all other analytes, chromatographic peak areas are plotted in place of analyte concentrations in Figure 1. For diatrizoate, a Spherisorb ODS-2 column (4.6×150 mm, 5 µm C-18 packing material; Waters) and 10 mm guard column of the same material was used as the stationary phase, and the mobile phase was a mixture of 20 mM phosphate buffer, 5 mM triethylamine and 5% methanol delivered isocratically at 1 mL/min. For iopromide, the stationary phase was a Novapak column (3.9×150 mm, 4 µm C-18 packing material; Waters) and 10 mm guard column of the same material. A gradient method (1 mL/min) was used with 5 mM ammonium acetate buffer (eluent A) and acetonitrile (eluent B): 4% eluent B was maintained for three minutes, then increased linearly to 7.5% at 10 min and held constant until 15 min, at which time it was decreased linearly back to 4% at 18 min and held constant for two additional minutes to re-equilibrate the column. As previously reported (1-3), doublet HPLC peaks are observed for iopromide (Iop-I₃) and its partially dehalogenated intermediates (Iop-HI₂ and Iop-H₂I) due to stereoisomerism; both peaks in each doublet were integrated to determine Iop-I₃ concentrations and to plot chromatographic peak areas for Iop-HI₂ and Iop-H₂I shown in Figure 1. With these methods, diatrizoate and iopromide concentrations down to 1 µM could be reliably detected.

Liquid chromatography-mass spectroscopy (LC-MS) was used to identify unknown organic reaction intermediates and products. Analysis was conducted on a Thermo Finnigan LCQ DecaXP system outfitted with a Thermo Surveyor HPLC system. Separation was accomplished using the Novapak column described above. For samples with diatrizoate and its products, a 5 µM ammonium acetate buffer was delivered isocratically at 1 mL/min over 10 minutes. For samples with iopromide and its products, a gradient method similar to the iopromide HPLC gradient method was applied, except that eluent A was 5 µM ammonium acetate. MS analyses were conducted in positive mode electrospray ionization and an ion trap mass spectrometer was used to separate ions over a mass range of 100–650 m/z for diatrizoate and 100-850 m/z for iopromide.

Iodide was quantified by ion chromatography with conductivity detection, using a Dionex ICS-2000 analyzer and an AS-18 column (Dionex IonPac). A mobile phase consisting of 36 mM KOH was delivered at 1 mL/min. Elemental analysis of the catalysts was conducted via inductively coupled plasma-mass spectrometry (ICP-MS) following high pressure, high temperature microwave digestion in nitric and hydrochloric acids. Filtered wastewater effluent and GAC-treated effluent samples were analyzed for dissolved organic carbon, using a Dohrmann Phoenix 8000 UV-persulfate analyzer.

Section S3: LC-MS Results and Analysis

Analyzing samples with HPLC revealed two intermediate peaks and one final product peak for both diatrizoate and iopromide. To ascertain the identity of these intermediates and products, LC-MS was conducted to identify the mass to charge ratio (m/z value) of each peak. **Figures SI-1** shows HPLC-UV chromatograms for samples collected from batch reactors during the Pd-catalyzed reduction of diatrizoate and iopromide. Individual peaks were identified by liquid chromatography-mass spectroscopy (LC-MS). **Figures SI-2** and **SI-3** show mass spectra collected for individual chromatogram peaks. For each ICM, the four mass peaks are separated by multiples of 126 m/z (the mass of I⁻ released, minus the mass of H⁺ added during each sequential dehalogenation step). For both diatrizoate and iopromide, the major peaks associated with each analyte have a m/z value corresponding to the ammonium ion adducts (formed during ionization in the ammonium acetate eluent), as well as minor peaks corresponding to the hydrogen ion adducts. The ring location where iodine is liberated during each of the sequential deiodination steps could not be determined from the LC-MS spectra. MS/MS spectra would be useful for making such assignments if the ICM fragments included a side chain and attached iodide, but poor fragmentation (mostly loss of additional iodine substituents) resulted in little meaningful data. Therefore, structures of intermediates shown in eqs 1-2 are accurate with respect to the number of iodine substituents remaining, but not necessarily the location of the remaining iodine substituents on the aromatic ring.

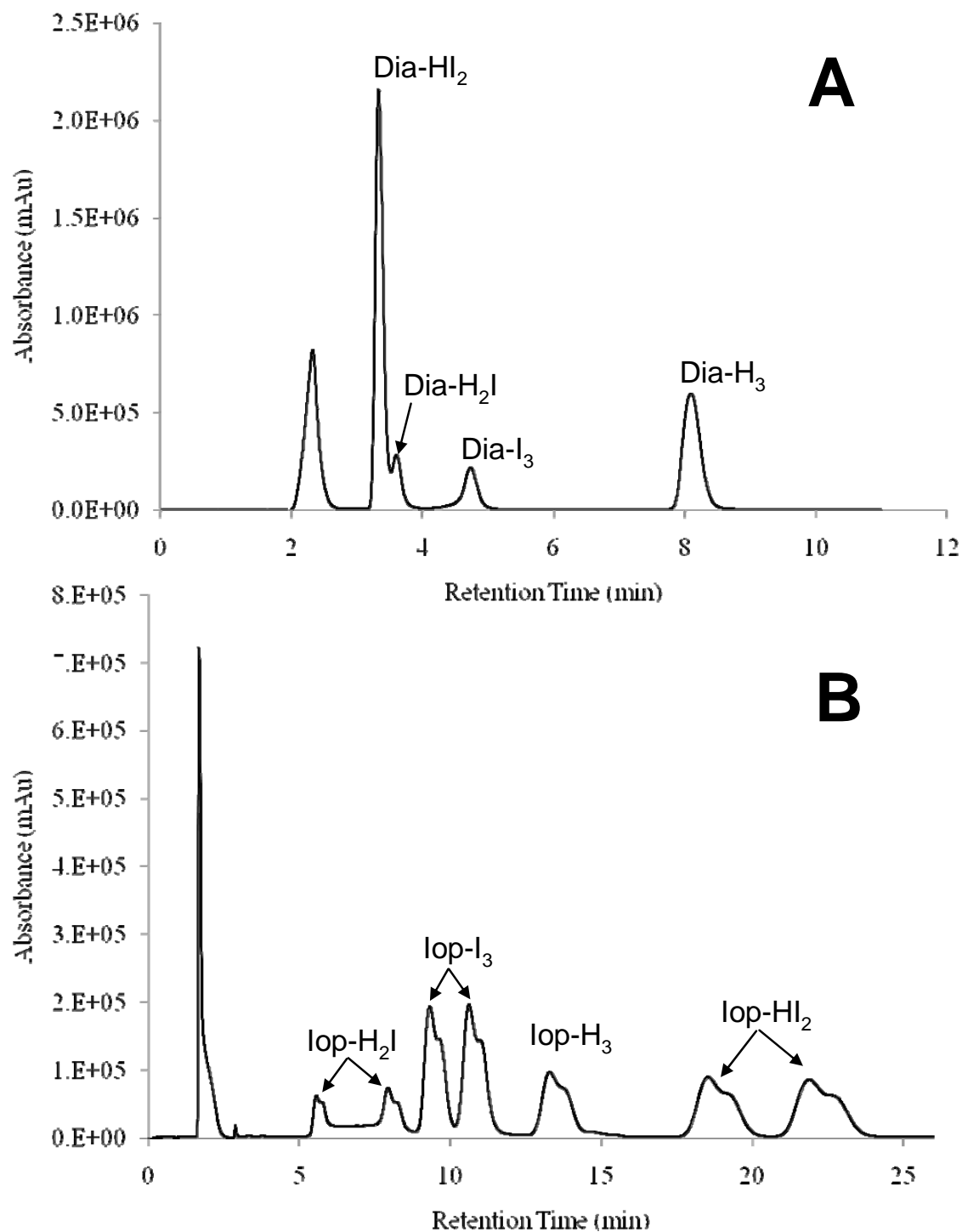


Figure SI-1. HPLC-UV chromatograms collected during Pd-catalyzed reduction of diatrizoate (A) and iopromide (B). Chromatograms correspond to samples collected to $t = 15$ min that are shown in Figure 1. Diatrizoate and iopromide chromatograms collected at $\lambda = 237$ nm and $\lambda = 241$ nm, respectively. Individual peak identities determined from associated mass spectra shown in Figure SI-2 and SI-3. Doublet peaks are observed for iopromide and associated reaction intermediates due to stereoisomerism (*1-3*).

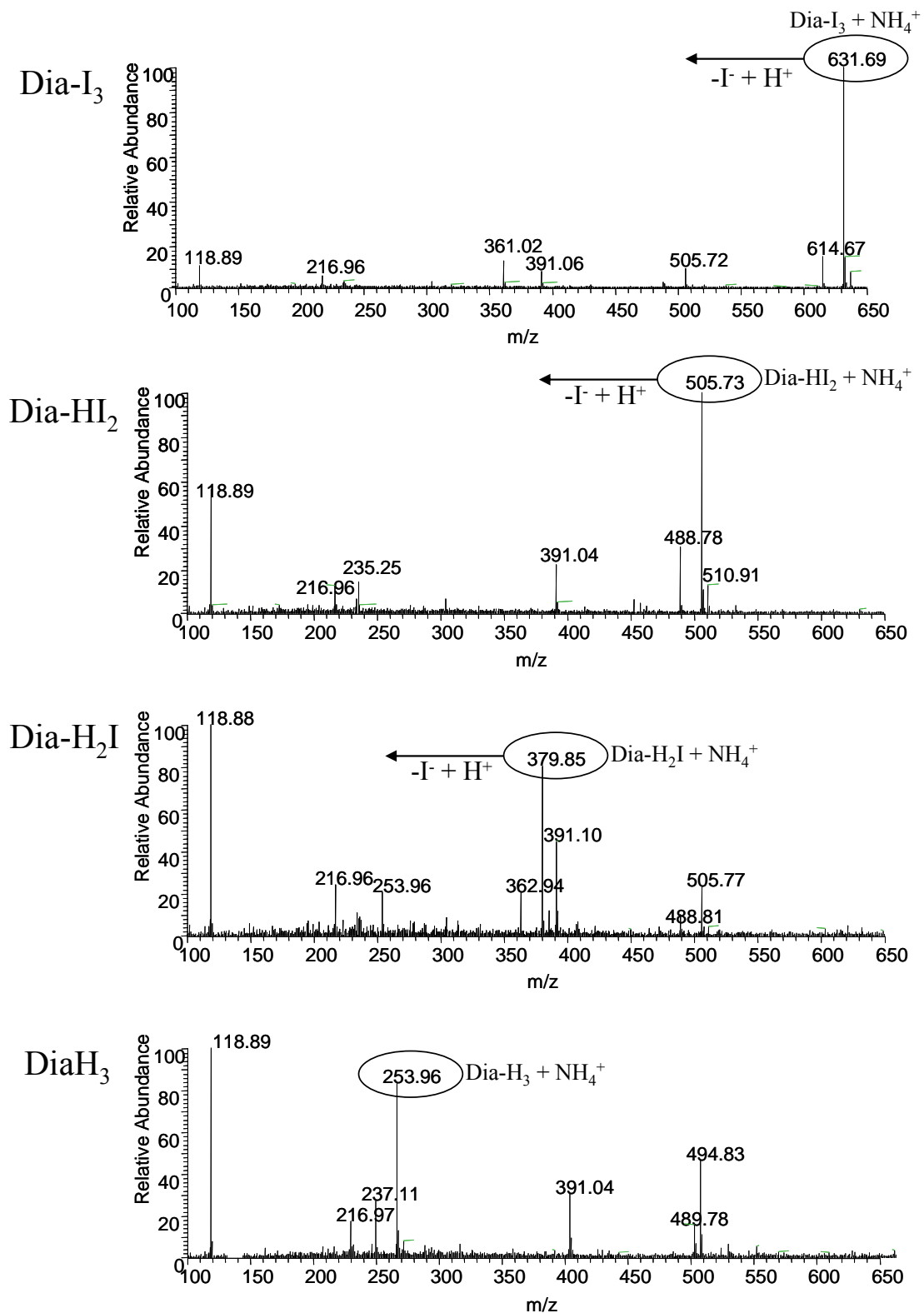


Figure SI-2. Mass spectra for diatrizoate and its sequential reduction products. Major peaks for the ammonium ion adducts are labeled. Peaks at $m/z = 119$ and $m/z = 217$ are present in background samples and can be neglected.

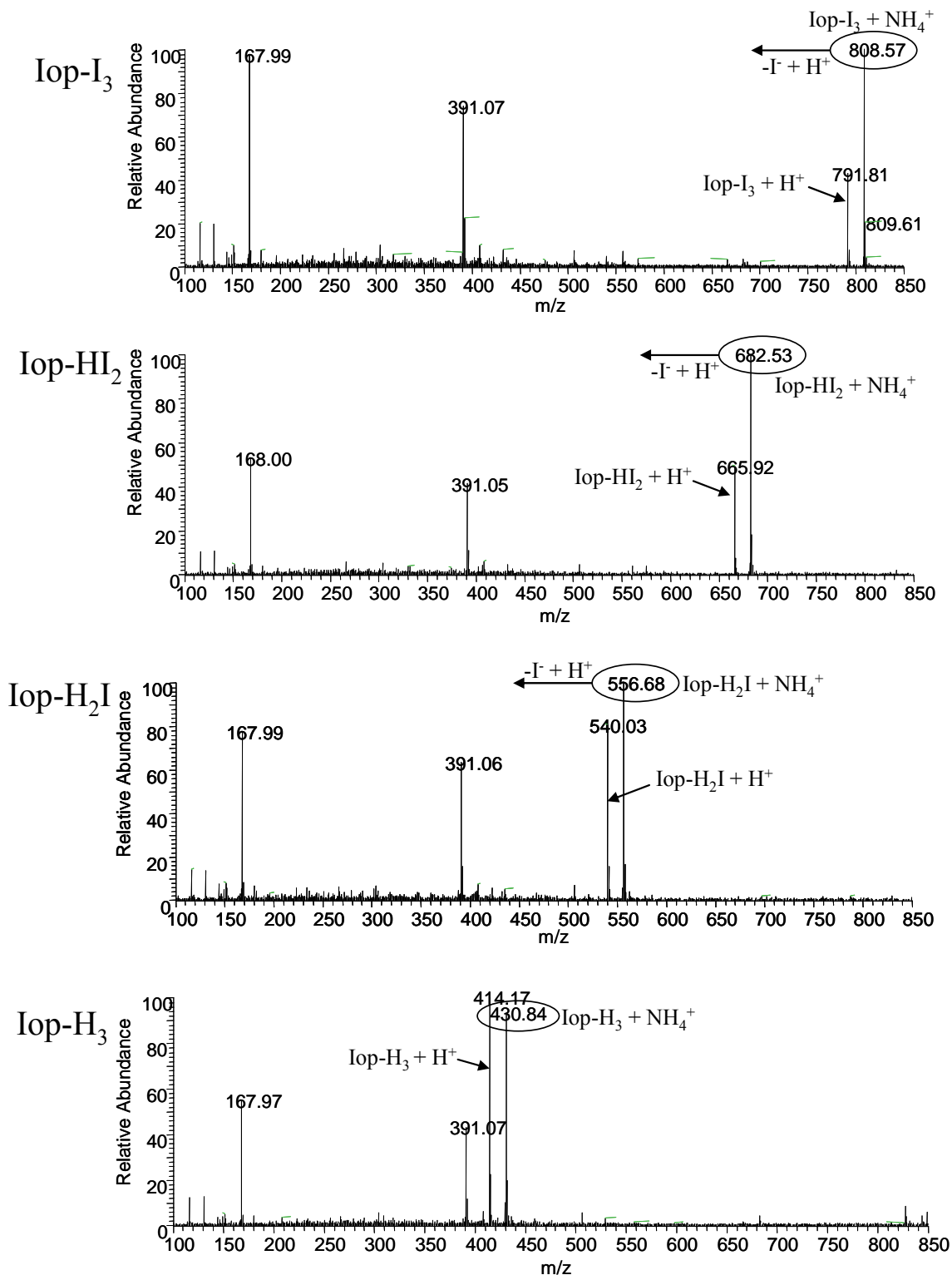


Figure SI-3. Mass spectra for iopromide and its sequential reduction products. Major peaks for the ammonium and hydrogen ion adducts of each analyte are labeled. Peaks at $m/z = 168$ and $m/z = 391$ are present in background samples and can be neglected.

Section S4. Results from Batch Kinetic Studies

Table SI-1. Summary of Results from Batch Kinetic Studies of Metal-Catalyzed Hydrodehalogenation of ICMs

Catalyst	Target ICM	[ICM] ₀ (μM)	M_{cat} ($\text{mg}_\text{M} \text{L}^{-1}$)	pH	Solution ^a Constituent	Constituent Concentration (mM)	k_{obs} (s^{-1}) ^b	r_o ($\mu\text{M} \text{s}^{-1}$) ^b
5wt% Pd/Al ₂ O ₃	diatrizoate	20	0.29	7.0	-	-	$2.70 (\pm 0.95) \times 10^{-4}$	$4.09 (\pm 0.57) \times 10^{-3}$
		20	0.57	7.0	-	-	$8.48 (\pm 1.04) \times 10^{-4}$	$1.10 (\pm 0.26) \times 10^{-2}$
		20	1.43	7.0	-	-	$2.68 (\pm 1.49) \times 10^{-3}$	$3.19 (\pm 1.20) \times 10^{-2}$
		20	2.85	7.0	-	-	$6.63 (\pm 1.05) \times 10^{-3}$	$6.97 (\pm 0.61) \times 10^{-2}$
		20	5.70	7.0	-	-	$1.50 (\pm 0.52) \times 10^{-2}$	$1.30 (\pm 0.07) \times 10^{-1}$
		20	8.55	7.0	-	-	$2.88 (\pm 0.88) \times 10^{-2}$	$1.85 (\pm 0.43) \times 10^{-1}$
		4	1.43	7.0	-	-	$6.22 (\pm 1.94) \times 10^{-3}$	$1.83 (\pm 0.15) \times 10^{-2}$
		100	1.43	7.0	-	-	$2.03 (\pm 0.53) \times 10^{-3}$	$1.13 (\pm 0.11) \times 10^{-1}$
		500	1.43	7.0	-	-	$6.63 (\pm 2.54) \times 10^{-4}$	$1.69 (\pm 0.58) \times 10^{-1}$
		1500	1.43	7.0	-	-	$2.71 (\pm 2.81) \times 10^{-4}$	$1.82 (\pm 0.49) \times 10^{-1}$
		2500	1.43	7.0	-	-	$6.67 (\pm 4.16) \times 10^{-5}$	$1.40 (\pm 0.65) \times 10^{-1}$
		20	1.43	3.2	-	-	$2.35 (\pm 1.56) \times 10^{-3}$	$3.86 (\pm 2.48) \times 10^{-2}$
		20	1.43	5.0	-	-	$4.21 (\pm 3.02) \times 10^{-3}$	$4.97 (\pm 3.24) \times 10^{-2}$
		20	1.43	9.0	-	-	$2.27 (\pm 1.26) \times 10^{-3}$	$3.05 (\pm 1.00) \times 10^{-2}$
		20	1.43	10.8	-	-	$1.91 (\pm 0.58) \times 10^{-3}$	$2.86 (\pm 0.64) \times 10^{-2}$
		20	1.43	7.0	ClO ₄ ⁻	50	$2.74 (\pm 0.72) \times 10^{-3}$	$3.87 (\pm 0.44) \times 10^{-2}$
		20	1.43	7.0	F ⁻	50	$2.01 (\pm 0.39) \times 10^{-3}$	$3.13 (\pm 0.43) \times 10^{-2}$
		20	1.43	7.0	Cl ⁻	50	$2.31 (\pm 1.00) \times 10^{-3}$	$3.39 (\pm 1.13) \times 10^{-2}$
		20	1.43	7.0	Br ⁻	50	$2.06 (\pm 0.50) \times 10^{-3}$	$3.19 (\pm 0.56) \times 10^{-2}$
		20	1.43	7.0	Mg ²⁺	10	$2.37 (\pm 0.77) \times 10^{-3}$	$3.47 (\pm 0.69) \times 10^{-2}$
		20	1.43	7.0	Ca ²⁺	10	$2.29 (\pm 0.53) \times 10^{-3}$	$3.09 (\pm 1.31) \times 10^{-2}$
		20	1.43	7.0	SO ₄ ²⁻	10	$1.70 (\pm 0.49) \times 10^{-3}$	$2.57 (\pm 0.92) \times 10^{-2}$
		20	1.43	7.0	NO ₃ ⁻	10	$1.94 (\pm 0.15) \times 10^{-3}$	$2.77 (\pm 1.12) \times 10^{-2}$
		20	1.43	7.0	HCO ₃ ⁻	10	$2.13 (\pm 0.46) \times 10^{-3}$	$3.28 (\pm 0.92) \times 10^{-2}$

Table SI-1. Continued

Catalyst	Target ICM	[ICM] ₀ (μM)	M_{cat} ($\text{mg}_\text{M} \text{L}^{-1}$)	pH	Solution ^a Constituent	Constituent Concentration (mM)	k_{obs} (s^{-1}) ^b	r_o ($\mu\text{M} \text{s}^{-1}$) ^b
5wt% Pd/Al ₂ O ₃	diatrizoate	20	1.43	7.0	I ⁻	0.4	$1.64 (\pm 1.31) \times 10^{-3}$	$2.53 (\pm 1.75) \times 10^{-2}$
		20	1.43	7.0	I ⁻	2	$1.02 (\pm 0.67) \times 10^{-3}$	$1.43 (\pm 0.41) \times 10^{-2}$
		20	1.43	7.0	I ⁻	10	$7.91 (\pm 2.50) \times 10^{-4}$	$1.36 (\pm 0.98) \times 10^{-2}$
		20	1.43	7.0	I ⁻	50	$5.78 (\pm 1.84) \times 10^{-4}$	$6.63 (\pm 0.72) \times 10^{-3}$
		20	1.43	7.0	S ²⁻	0.1	$3.92 (\pm 0.23) \times 10^{-4}$	$5.92 (\pm 2.37) \times 10^{-3}$
		20	1.43	7.0	S ²⁻	1	$1.69 (\pm 3.22) \times 10^{-5}$	$3.85 (\pm 4.01) \times 10^{-4}$
		20	1.43	7.0	S ²⁻	10	NR ^e	NR ^e
		20	1.43	7.0	NOM	1 mg L ⁻¹	$1.71 (\pm 0.90) \times 10^{-3}$	$2.14 (\pm 0.96) \times 10^{-2}$
		20	1.43	7.0	NOM	5 mg L ⁻¹	$8.83 (\pm 3.78) \times 10^{-4}$	$1.35 (\pm 0.54) \times 10^{-2}$
		20	1.43	7.0	NOM	25 mg L ⁻¹	$2.83 (\pm 1.15) \times 10^{-4}$	$3.69 (\pm 3.12) \times 10^{-3}$
		20	1.43	7.0	filtered WW effluent ^c		2.82×10^{-4}	6.56×10^{-3}
		20	1.43	7.0	filtered/GAC-treated WW effluent ^d		1.56×10^{-3}	1.67×10^{-2}
	iopromide	20	0.29	7.0	-	-	$2.89 (\pm 1.67) \times 10^{-4}$	$4.76 (\pm 2.61) \times 10^{-3}$
		20	0.57	7.0	-	-	$8.25 (\pm 2.07) \times 10^{-4}$	$1.06 (\pm 0.34) \times 10^{-2}$
		20	1.43	7.0	-	-	$2.54 (\pm 0.45) \times 10^{-3}$	$2.84 (\pm 0.24) \times 10^{-2}$
		20	2.85	7.0	-	-	$6.26 (\pm 2.10) \times 10^{-3}$	$5.92 (\pm 1.33) \times 10^{-2}$
		20	5.70	7.0	-	-	$1.79 (\pm 0.10) \times 10^{-2}$	$1.34 (\pm 0.13) \times 10^{-1}$
		20	8.55	7.0	-	-	$3.40 (\pm 0.27) \times 10^{-2}$	$1.96 (\pm 0.88) \times 10^{-1}$
1wt% Pd/Al ₂ O ₃	diatrizoate	20	0.05	7.0	-	-	$1.13 (\pm 0.87) \times 10^{-4}$	$2.71 (\pm 0.16) \times 10^{-3}$
		20	0.09	7.0	-	-	$5.33 (\pm 1.73) \times 10^{-4}$	$7.41 (\pm 2.62) \times 10^{-3}$
		20	0.23	7.0	-	-	$1.71 (\pm 0.58) \times 10^{-3}$	$2.09 (\pm 0.39) \times 10^{-2}$
		20	0.46	7.0	-	-	$4.29 (\pm 1.17) \times 10^{-3}$	$4.61 (\pm 0.61) \times 10^{-2}$
		20	0.92	7.0	-	-	$1.03 (\pm 0.33) \times 10^{-2}$	$1.00 (\pm 0.16) \times 10^{-1}$
		20	1.43	7.0	-	-	$2.13 (\pm 0.72) \times 10^{-2}$	$2.31 (\pm 2.37) \times 10^{-1}$
Pd/Cu/Al ₂ O ₃	diatrizoate	20	1.43	7.0	-	-	$1.21 (\pm 0.98) \times 10^{-3}$	$1.42 (\pm 1.04) \times 10^{-2}$
Pd/In/Al ₂ O ₃	diatrizoate	20	1.43	7.0	-	-	$1.04 (\pm 0.33) \times 10^{-3}$	$1.22 (\pm 0.59) \times 10^{-2}$

Table SI-1. Continued

Catalyst	Target ICM	[ICM] ₀ (μM)	<i>M</i> _{cat} (mg _M L ⁻¹)	pH	Solution ^a Constituent	Constituent Concentration (mM)	Washing Solution	<i>k</i> _{obs} (s ⁻¹) ^b	<i>r</i> ₀ (μM s ⁻¹) ^b
porous Ni	diatrizoate	20	222.5	7.0	-	-	-	5.68 (±1.34) x 10 ⁻³	4.28 (±4.01) x 10 ⁻²
		20	445.0	7.0	-	-	-	9.19 (±2.53) x 10 ⁻³	7.61 (±7.11) x 10 ⁻²
		20	667.5	7.0	-	-	-	1.04 (±0.65) x 10 ⁻²	8.63 (±6.02) x 10 ⁻²
		20	890.0	7.0	-	-	-	2.07 (±0.41) x 10 ⁻²	1.88 (±0.44) x 10 ⁻¹
		20	1112.5	7.0	-	-	-	2.41 (±0.64) x 10 ⁻²	1.94 (±0.09) x 10 ⁻¹
		20	1335.0	7.0	-	-	-	2.98 (±0.99) x 10 ⁻²	1.94 (±0.26) x 10 ⁻¹

Catalyst-Regeneration Experiments

5wt% Pd/Al ₂ O ₃	diatrizoate	20	1.43	7.0	I ⁻	10	-	7.91 (±2.50) x 10 ⁻⁴	1.36 (±0.98) x 10 ⁻²
		20	1.43	7.0	I ⁻	10	None ^f	2.08 (±0.69) x 10 ⁻³	2.15 (±0.28) x 10 ⁻²
		20	1.43	7.0	I ⁻	10	Water ^g	2.35 (±0.83) x 10 ⁻³	2.45 (±0.41) x 10 ⁻²
		20	1.43	7.0	S ²⁻	1	-	1.69 (±3.22) x 10 ⁻⁵	3.85 (±4.01) x 10 ⁻⁴
		20	1.43	7.0	S ²⁻	1	Water ^g	1.93 (±2.86) x 10 ⁻⁴	2.56 (±1.79) x 10 ⁻³
		20	1.43	7.0	S ²⁻	1	NaOCl ^h	1.16 (±1.67) x 10 ⁻³	7.32 (±2.37) x 10 ⁻³
		20	1.43	7.0	NOM	5 mg L ⁻¹	-	8.83 (±3.78) x 10 ⁻⁴	1.35 (±0.54) x 10 ⁻²
		20	1.43	7.0	NOM	5 mg L ⁻¹	Water ^g	1.92 (±1.02) x 10 ⁻⁴	2.86 (±0.18) x 10 ⁻³
		20	1.43	7.0	NOM	5 mg L ⁻¹	NaOCl ^h	6.15 (±3.36) x 10 ⁻⁴	8.40 (±1.12) x 10 ⁻³
		20	1.43	7.0	NOM	5 mg L ⁻¹	Alkaline ⁱ	2.39 (±0.47) x 10 ⁻³	2.40 (±0.29) x 10 ⁻²

^a Cationic solution constituents added as chloride salts and anionic constituents added as sodium salts. NOM = Suwanee River natural organic matter reverse osmosis isolate obtained from the International Humic Substances Society. ^b Parameters and uncertainties represent averages and 95% confidence levels calculated from triplicates. Replicates were not measured if no measure of uncertainty is provided. Initial reaction rate determined from the slope of [ICM] vs. time plots. ^c Wastewater effluent filtered through a glass fiber filter and 0.1 μm hydrophilic PVDF filter to remove suspended solids. ^d Filtered wastewater effluent (4.9 mg/L DOC) was passed through a column of granular activated carbon with residence time >20 min to remove NOM (1.3 mg/L DOC in the GAC-treated effluent). ^e No reaction observed. ^f Air-dried catalyst collected after exposing to foulant-containing solution was not exposed to regenerants or water until re-suspending in deionized water and adding diatrizoate to initiate the reaction. ^g Air-dried catalyst collected after exposing to foulant was stirred in 500 mL deionized water for two hours, then rinsed with an additional 2 L water and air-dried for 3 days, then re-suspended in deionized water before measuring reaction with diatrizoate. ^h Air-dried catalyst collected after exposing to foulant was stirred in 500 mL of aqueous solution containing 28 mM NaOCl (pH 7.8) for two hours, then rinsed with 2 L water and air-dried for 3 days, then re-suspended in deionized water before measuring reaction with diatrizoate. ⁱ Air-dried catalyst collected after exposing to foulant was stirred in 500 mL of pH 11 aqueous solution (water adjusted with 1 M NaOH) for two hours, then rinsed with 2 L water and air-dried for 3 days, then re-suspended in deionized water before measuring reaction with diatrizoate.

Section S5: Calculation of Weisz-Modulus Φ

The dimensionless Weisz-modulus Φ (4) can be used to estimate the importance of intraparticle diffusion resistance to observed catalytic reaction rates:

$$\Phi = \frac{k_{obs} L^2}{D_{eff}} \quad (s1)$$

where k_{obs} is the measured pseudo-first-order rate constant, L is the characteristic diffusion pathlength for the catalyst and D_{eff} is the effective molecular diffusion coefficient of the reacting solute. Eq 1 provides a general measure of the characteristic time scale for pore diffusion relative to the observed characteristic time scale of the reaction. A calculated value of $\Phi \ll 1$ indicates that diffusion is fast compared to the observed reaction, whereas $\Phi > 1$ indicates that pore diffusion may be limiting.

We determined Φ for diatrizoate reacting with the 5%Pd/Al₂O₃ catalyst, using conservative estimates that enhance the likelihood that the calculated value $\Phi > 1$. We used the largest measured value of k_{obs} ($2.88 \times 10^{-2} \text{ s}^{-1}$). For spherical particles, L is equal to 1/6 of the particle diameter, and the largest possible catalyst particles were 38 μm because only catalyst particles passing through a #400 sieve were used in kinetic experiments. Thus,

$$L = \frac{1}{6} d_p = \frac{1}{6} (38 \times 10^{-6} \text{ m}) = 6.3 \times 10^{-6} \text{ m} \quad (s2)$$

The molecular diffusion coefficient of diatrizoate (D_{mol}) in water was estimated using the method in Hayduk and Laudie (5):

$$D_{mol} = \frac{13.26 \times 10^{-5}}{\mu^{1.14} (\nu')^{0.589}} \quad (s3)$$

where D_{mol} is in units of $\text{cm}^2 \text{ s}^{-1}$, μ is the absolute viscosity of water in units of $\text{g m}^{-1} \text{ s}^{-1}$, and ν' is the molal volume of the reacting solute in $\text{cm}^3 \text{ mol}^{-1}$, which was calculated using the LeBas incremental method (**Table SI-2**):

Table SI-2. Calculation of the Molal Volume of Diatrizoate			
Diatrizoate	<u>Atomic Volume</u>	<u>Number</u>	<u>Total</u>
iodine	37	3	111
double-bonded oxygen	7.4	3	22.2
secondary amine nitrogen	12	2	24
oxygen	12.8	1	12.8
carbon	14.8	11	162.8
hydrogen	3.7	9	33.3
correction for benzene ring	-15	1	-15
$\nu' =$			351.1

Plugging the results from Table SI-2 into eq s3, and using $\mu = 1.002 \text{ g m}^{-1} \text{ s}^{-1}$ (at 20°C), we obtained an estimate for D_{mol} :

$$D_{mol} = \frac{13.26 \times 10^{-5}}{(1.002)^{1.14} (351.1)^{0.589}} = 4.19 \times 10^{-6} \text{ cm}^2 \text{ s}^{-1} = 4.19 \times 10^{-10} \text{ m}^2 \text{ s}^{-1}$$

As a conservatively low estimate, the effective diffusion coefficient of diatrizoate inside the porous support particle was approximated as 1/10 of its value in water (6):

$$D_{eff} = 4.19 \times 10^{-11} \text{ m}^2 \text{ s}^{-1}$$

Then, plugging these values into eq s1 yields a value of 2.7×10^{-2} for Φ :

$$\Phi = \frac{k_{obs} L^2}{D_{eff}} = \frac{(2.88 \times 10^{-2} \text{ s}^{-1}) (6.3 \times 10^{-6} \text{ m})^2}{4.19 \times 10^{-11} \text{ m}^2 \text{ s}^{-1}} = 2.7 \times 10^{-2}$$

Because the calculated value of $\Phi \ll 1$, intraparticle mass transfer resistance is assumed to be negligible on the time scale over which diatrizoate reduction is observed.

Section S6: Supplemental Plots of Kinetic Data

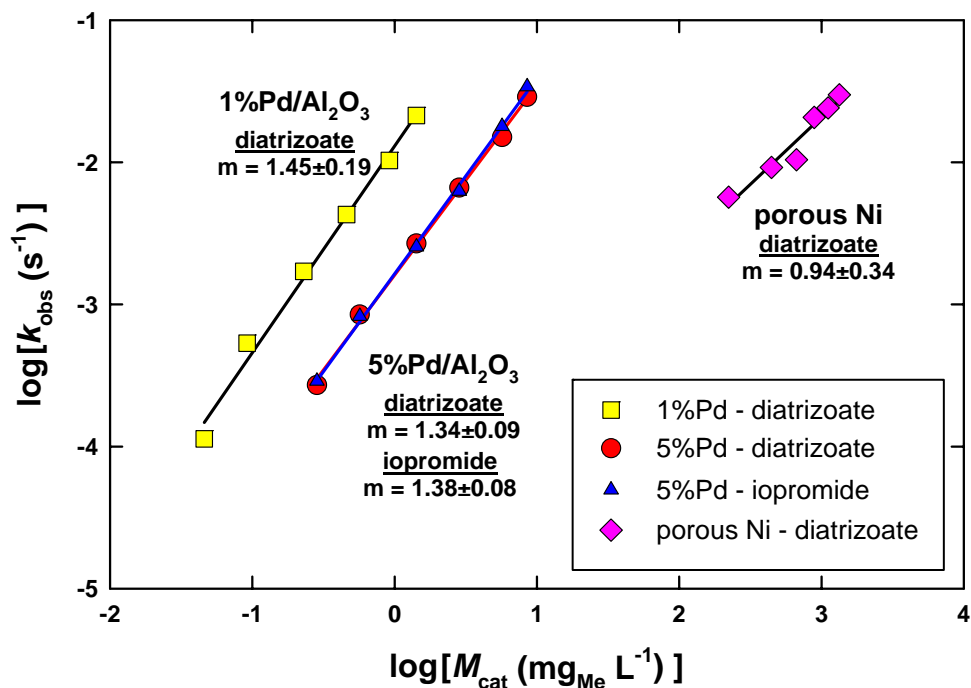


Figure SI-4. Apparent reaction order plots for metal-catalyzed hydrodehalogenation of ICM with respect to active metal loading (M_{cat}) of Pd and Ni catalysts. Measured slopes indicate apparent reaction order. Reaction conditions: $[\text{ICM}]_0 = 20 \mu\text{M}$, $0.046\text{--}8.55 \text{ mg}_{\text{Pd}} \text{L}^{-1}$, $225\text{--}1335 \text{ mg}_{\text{Ni}} \text{L}^{-1}$, $P_{\text{H}_2} = 0.1 \text{ MPa}$, pH 7.0, 25 °C.

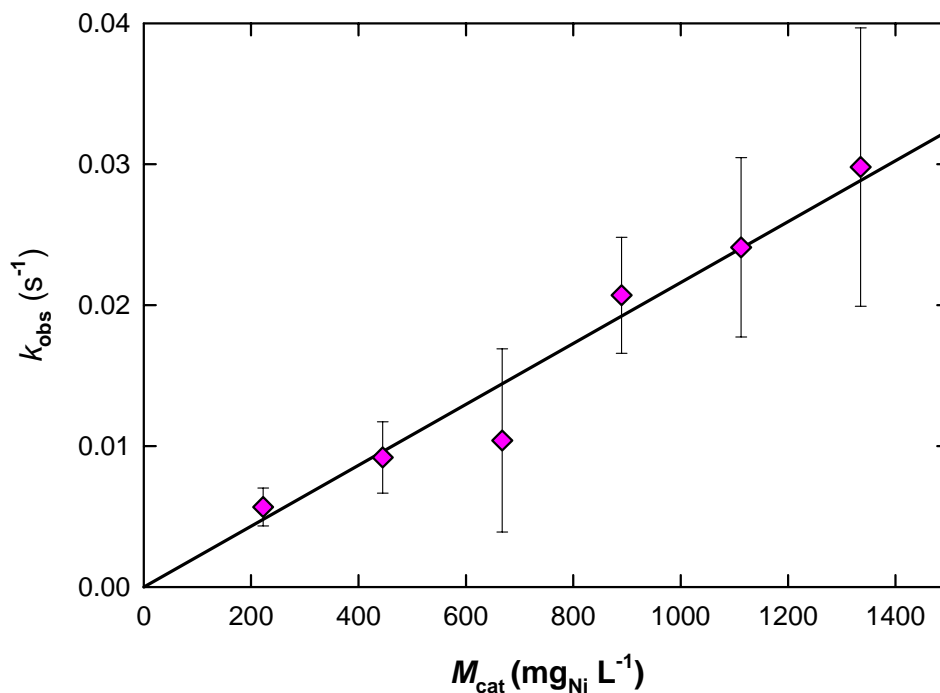


Figure SI-5. Effect of Ni catalyst loading on the pseudo-first-order rate constant for hydrodehalogenation of diatrizoate. Error bars indicate 95% confidence level calculated from triplicate averages. Line indicates linear regression with intercept through zero. Reaction conditions: $[\text{diatrizoate}]_0 = 20 \mu\text{M}$, $225\text{--}1335 \text{ mg}_{\text{Ni}} \text{L}^{-1}$, $P_{\text{H}_2} = 0.1 \text{ MPa}$, pH 7.0, 25 °C.

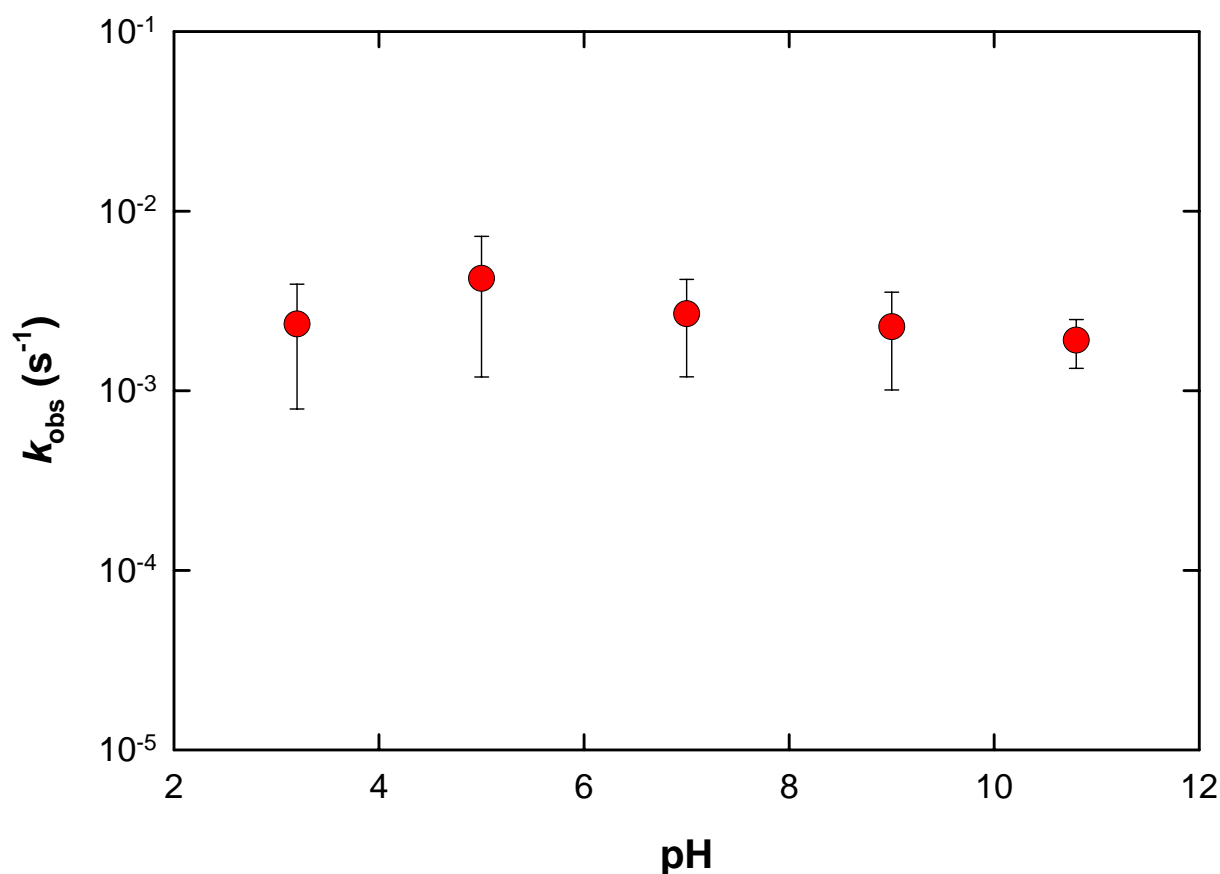


Figure SI-6. Effect of pH on Pd-catalyzed hydrodehalogenation of diatrizoate. Error bars represent 95% confidence level calculated from triplicate averages. Reaction conditions: $[\text{diatrizoate}]_0 = 20 \mu\text{M}$, $1.43 \text{ mg}_{\text{Pd}} \text{ L}^{-1}$ (5%Pd/ Al_2O_3), $P_{\text{H}_2} = 0.1 \text{ MPa}$, 25°C .

References Cited in Supporting Information Section

- (1) Perez, S.; Eichhorn, P.; Celiz, M. D.; Aga, D. S. Structural characterization of the metabolites of the X-ray contrast agent iopromide in activated sludge using ion trap mass spectrometry. *Anal. Chem.* **2006**, *78*, 1866-1874.
- (2) Dunn, J.; Lin, Y.; Miller, D.; Rogic, M.; Neumann, W.; Woulfe, S.; White, D. Stereoisomerism in contrast media Ioversol. *Invest. Radiol.* **1990**, *25*, S102-S103.
- (3) Putschew, A.; Wischnack, S.; Jekel, M. Occurrence of triiodinated X-ray contrast agents in the aquatic environment. *Sci. Tot. Environ.* **2000**, *255*, 129-134.
- (4) Weiz, P. B.; Prater, C. D. Interpretation of measurements in experimental catalysis. *Adv. Catal.* **1954**, *6*.
- (5) Harriott, P. Mass transfer to particles: Part I. Suspended in agitated tanks. *AIChE J.* **1962**, *8*, 93-101.
- (6) Mackenzie, K.; Frenzel, H.; Kopinke, F.-D. Hydrodehalogenation of halogenated hydrocarbons in water with Pd catalysts: Reaction rates and surface competition. *Appl. Catal. B* **2006**, *63*, 161-167.